Improved Gas Separation of PEBAX-CSWCNTs Mixed Matrix Membranes

Pouria Abbasszadeh Gamali[1,2], Mohammadreza Rahmani[1,3], Abbass Kazemi[1,*] and Mahnaz Pourkhalil[1]

[1]*Nanotechnology and Carbon Research Center, Research Institute of Petroleum Industry (RIPI), Tehran, Iran*

[2]*Chemistry & Chemical Engineering Research Center of Iran, Tehran, Iran*

[3]*Department of Chemical Engineering, Babol Noshirvani University of Technology, Babol, Iran*

Abstract: In the present study, mixed matrix membranes (MMMs) were prepared using PEBAX[®] 3000 as polymer matrix and single-wall carbon nanotubes (SWCNTs) functionalized with carboxyl groups as nanofillers. The effects of the nanofillers on separation of CO_2/N_2 and CO_2/CH_4 were investigated. The pristine PEBAX membrane indicated gas selectivity values of 23 and 13 for CO_2/N_2 and CO_2/CH_4, respectively. However selectivity of the modified membrane for gas pairs of CO_2/N_2 and CO_2/CH_4 improved to the values of 106.4 and 31.3, respectively. In other words, selectivity of modified membranes compared to those of unmodified ones enhanced greatly. The dramatic increase in gas selectivity of the mixed matrix membranes can be attributed to the polar groups of caboxyl-functionalized single-wall carbon nanotubes (CSWCNTs). While CO_2 permeability of MMMs increaesd, permeability of nonpolar gases (N_2 and CH_4) decreased. FTIR spectra depicted that there were inter/intramolecular forces between ether and amide groups of the polymer chains. For PEBAX membrane filled with 10 wt% CSWCNTs, the peaks of C-O-C، N-H, and H-N-C=O functional groups shifted to lower values due to the formation of hydrogen bonds between polar carboxyl groups of CSWCNTs and amide/ether groups of PEBAX copolymer. Relative crystallinity values of the membranes with various CSWCNTs content were calculated using ΔH_f data obtained from DSC measurements. Results demonstared that the rise in content of CSWCNTs brought about the decrement in crystallinity values of polyamide segments. The morphology of the membrane containing 10 wt% CSWCNTs was also investigated emplying AFM images, and a suitable compatability and adhere between PEBAX and CSWCNTs was last confirmed.

Keywords: Mixed matrix membranes (MMMs), Poly(ether-block-amide), Nanofillers, Permselectivity, Gas separation.

1. INTRODUCTION

In recent years, mixed matrix membranes (MMMs) have been immensely studied because of their capabilities to be utilized in a wide range of applications in gas separation technology. In general, polymer membranes are economically of more interest than other types of membranes because of their easily processability [1-7]. Cellulose acetate, Polyimides, Polyethylene glycol, to name just a few, used to apply in order to prepare membranes [8]. What is more, enhanced permselectivity of membranes can be achieved by chemical modification. Tailored-functional membranes can be made using nanomaterials incorporated into the polymer matrix, leading to hybrid membranes preparation with improved chemical and physical properties. In most cases, MMMs indicate both higher gas permeabilities and better gas selectivities compared to those of pristine membranes [9-12].

Poly (ether block amide), commercially known as PEBAX, is made up of two various segments including, linear chaines of rigid polyamide (PA) and flexible

polyether (PE). High mobility of PE segments makes permeability of gases through PEBAX way easier. The rubbery PE segments possess a glass transition temparature below room temperature and thus it makes polymer chains flexible. PA segments, however, can be crystallized at glass transition temperature above room temperature, so proper thermal and mechanial strength are provided for PEBAX membranes. It is worth noting that gases mainly transport through the amorphous PE phase. The compatibility of PEBAX and inorganic nanofillers has positive effects on mechanical and thermal properties of MMMs. The higher gas permeability and permselectivity were resulted from the hybrid membranes. The improved permeation properties can be attributed to the interactions between CO_2 molecules and SiO_2 nanoparticles within the polymer matrix. Moreover, additional sorption sites were provided in PE blocks of PEBAX at organic-inorganic interfaces. In order to produce MMMs, solution casting is a simple procedure whereby inorganic nanofillers can be dispersed whitin a polymer solution. Once solvent evaporates, MMMs will be formed on the bottom of petri dish. The high permeability and selectivity of PEBAX membranes can be attributed to the special affinity between polarizable gases and PE

*Address correspondence to this author at the Nanotechnology and Carbon Research Center, Research Institute of Petroleum Industry (RIPI), Tehran, Iran; Tel: 0098 21 48255404; Fax: 0098 21 44739696; E-mail: kazemiab@ripi.ir

segments in PEBAX chains. Kim *et al*. employed a sol-gel process for preparation of hybrid membrane of PEBAX/silica [13-16].

The effect of inorganic fillers on properties of MMMs is associated with their surface chemistry, chemical structure and size of particles. In general, inorganic fillers are divided into two distinct groups, porous and nonporous types. Each of the filler types has various effects on properties of MMMs. Porous fillers tend to act as a molecular sieving agent and separate gas components by their size. In fact, incorporation of porous fillers into polymer matrix raises permeability of desired gas component through membrane. Adding porous fillers can also increase selectivity of MMMs. As a result, the advantages of polymeric and inorganic fillers are combined by preparation of MMMs. Apart from molecular sieving, adding fillers possessing large pore size to polymer matrix can induce selective surface flow. It can be concluded that small and polar component (CO_2) can be adsorbed and diffused through the pores comfortably compared to the other components (N_2 and CH_4). Therefore, N_2 and CH_4 permeate more slowly than CO_2. Generally, the ways that nanofillers affect gas separation performance of MMMs can be gategorozed into by four various models, including Maxwell model, Free-volume increase, Solubility increase, and Nanogap hypothesis, which was thoroughly explianed in our previous study [1].

The primary focus of this study was to prepare super-permeable MMMs. Hence, PEBAX[®] 3000 and CSWCNTs were employed as polymer matrix and nanofillers, respectively, to fabricate composite membranes. The impact of polar nanofillers, playing a big part in rising gas selectivity, on both permeabilities of CO_2, N_2, and CH_4 and selectivitis of CO_2/N_2 and CO_2/CH_4 were examined. The enhanced CO_2/N_2 and CO_2/CH_4 selectivities were achieved which is a new record for PEBAX[®] 3000 membranes.

2. EXPERIMENTAL

2.1. Materials and Membranes Preparation

PEBAX[®] 3000 with a chemical structure as shown in Figure **1** and CSWCNTs were purchased from Arkema

and Nanocy, respectively. N,N'-dimethyl-acetamide (DMAc) as solvent was provided from Fluka and used as received. Pure gases were dedicated by research institute of petroleum industry (RIPI). Table **1** dipicts physical propertis of CSWCNTs.
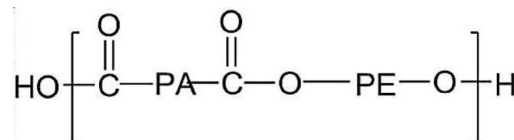

Figure 1: Chemical structure of PEBAX 3000.

A 2.6wt% polymer solution was prepared by dissolving 0.26g PEBAX in 9.74g DMAc under reflux (90°C), and the solution was stirred for 3h. In the next step, solution was poured into a petri dish placed on a flat hot-stage at 60-70°C in order to form a film at the bottom of petri dish. After about 90min, solvent completely evaporated and some distilled-water was subsequently poured into the petri dish and polymeric film was then separated from glass, and dried at room temperature. To ensure that no solvent remains within polymer matrix, fabricated membranes were placed in a vacuum oven at 90°C for 18h. For preparation of MMMs, the appropriate amount of CSWCNTs nanofillers were first dispersed in 9.74g DMAc and then placed in an ultrasonic apparatus for 1h to ensure that nanofillers were properly dispersed throughout the solvent. The suspension was last added to provided PEBAX solution, and composite membranes were fabricated using casting solution.

2.2. Membrane Characterization

2.2.1. Surface Morphology

Surface morphology of both pristine PEBAX membranes and MMMs were studied using AFM and SEM images. The AFM images were obtained using universal scanning probe microscope (SPM) analyzer, Solver P-47H AFM (NT-MDT, Russia). Moreover, elemental analysis and mapping of nanofillers distribution within polymer matrix were investigated employing SEM-EDX spectrometer. Cross-section morphology of the MMMs (consisting 10wt% CSWCNTs) was obtianed using field emission scanning electron microscopy (FESEM) MIRA TESCA model at voltage of 15kV.

Table 1: Physical Properties of Carboxylated Single Wall Carbon Nanotube

Length	Outer diameter	Inside diameter	Bulk density(g/cm³)	True density(g/cm³)	Specific surface area(m²/g)
30nm	1-2nm	0.8-1.6nm	0.14	~2.1	407

2.2.2. Thermal Characterestics

The thermal properties of samples were investigated using a differential scanning calorimetry (Perkin-Elmer DSC-7), from 30 ºC up to 250 ºC at the heating rate of 20 ºC/min under nitrogen purge. The crystallinity degree (X_c) of the membranes were determined using the following equation,

$$X_c (\%) = (\Delta H_f / \Delta H_f^0 \times w) \times 100 \qquad (1)$$

Where ΔH_f is the fusion enthalpy at the T_m and ΔH_f^0 is the fusion enthalpy of the 100% crystalline polymer (ΔH_f^0 = 246J/g for PA_{12} and 196.6J/g for PEO), and w stands for the weight percent of PA and PE phases in the block copolymer Pebax [17]. The thermal stability behaviour for all membranes were examined by a Perkin thermogravimetric analyzer, from 30 ºC to 1000 ºC and at the heating rate of 20 ºC/min rate under nitrogen purge. The weight loss (%) was recorded as a function of temperature.

2.2.3. Fourier Transform Infrared Spectroscopy

To study functional groups of polymer membranes, FTIR instrument ISS-88 Bruker model was employed. The typical IR spectrums were recorded in the range of 400-4000cm⁻¹.

2.2.4. Contact Angle Measurments

The contact angle measurements were applied to characterize the hydrophilic/hydrophobic behaviour of the membranes surface. The contact angle of the samples were measured using a sessile drop method. The static contact angles of water droplets on the upper surface of the samples, varying from 55° to 90° for pristine PEBAX membrane and from 40° to 75° for MMMs (containing 10wt% CSWCNTs), as a function of normalized time (60s) were recorded.

2.2.5. Determination of Density, Volume Fraction, Free Volume, Solubility Parameter, and Flory-Huggins Intraction

The experimental density of the samples were determined with respect to the standard buoyancy method. All samples were dried in vacuum oven at 30 ºC overnight. The experimental density, ρ_f (g/cm³) of the samples can be determined by the following equation [18],

$$\rho_f = \frac{wt_{air}}{wt_{air} - wt_{ax}} \times \rho_0 \qquad (2)$$

Where ρ_0 is the density of the auxilary liquid (hexane), wt_{air} is sample weight at room temperature,

and wt_{ax} is sample weight in the auxiliary liquid. The theoretical density of MMMs determined according to the additive model using the following equation [18],

$$\rho_f = \phi_1 \rho_1 + \phi_2 \rho_2 \qquad (3)$$

Where ρ_1 (2.1g/cm³) and ρ_2 (1.02g/cm³) are the densities of the CSWCNTs and PEBAX, respectively. ϕ_1 and ϕ_2 also present the volume fraction of the CSWCNTs and PEBAX, respectively. Volume fraction (ϕ_f) of prepared filmes can be calculated using the following equation,

$$\phi_f = \frac{W_f}{W_f + \left(\dfrac{\rho_f}{\rho_P} \times (1 - W_f) \right)} \qquad (4)$$

Where ρ_P and ρ_f stand for the densities of the PEBAX and CSWCNTs, respectivly, and W_f represents the CSWCNTs weight fraction. Free volume of a polymer is defined as the volume which is not occupied by atoms of polymer chains. A polymer with a high content of free volume can affect the diffusion coefficient of membranes, and gas molecules can diffuse through the voids. In the case of semi-crystalline polymers, including PEBAX, gas permeation normally occure through the amorphous region of the polymer. The high mobility of the amorphous polyether segments leads to a facile permeability of gases through the PE region [17]. Free volume of membranes can be calculated using the following Bondiʼs group contribution method [17],

$$FFV = \frac{v - v_0}{v} \qquad (5)$$

Where V (cm³/gr) is the specific volume of a polymer matrix (can be calculated from density), and V_0 (cm³/gr) is the van der Waals volume which can be calculated by the group contribution method as outlined in Bondi [19].

It is plainly visible that if two different materials have a similar solubility parameters, they can be fully miscible. Therefore, the solubility parameter plays an important role in the development of stable commercial chemical formulations. It is imperative to assess phase segregation during product synthesis. In 1950, the solubility parameter was first used by Hildebrand and Scott [20]. The Hildebrand solubility parameter of a substance is defined as the square root of the cohesive energy density (CED) at 298K for non-polar compounds. The solubility parameter is defined as follows [21],

$$\delta = (CED)^{1/2} \tag{6}$$

$$CED = \left(\frac{\Delta E_V}{V}\right) = \left(\frac{\Delta H_V - RT}{V}\right) \tag{7}$$

Where δ is a solubility parameter, ΔE_V is molar energy of vaporization, ΔH_V is molar heat of vaporization, and V is molar volume of a pure solvent. The measurment units are, $(cal/cm^3)^{1/2} = 0.4888 \times MPa^{1/2}$ and $MPa^{1/2} = 2.0455 \times (cal/cm^3)$.

Van der Waals interactions between solvent and polymer chains for a nonpolar system are generally well expressed by Flory–Huggins interaction parameter χ, which is expressed by equation below,

$$\chi_{12} = \chi_S + \chi_H \tag{8}$$

Where χ_S and χ_H are the entropic and enthalpic components of polymer-solvent interactions, respectively. The value of empirical factor (χ_S) generally for a nonpolar system is equal to 0.34. The relationship between the solubility parameter and the Flory–Huggins interaction parameter can be expressed using the following equation [21],

$$\chi_H = \frac{V_s}{RT}(\delta_1 - \delta_2)^2 \tag{9}$$

Where V_s stands for solvent molar volume, R refers to ideal gas constant (8.314J/mol), T is the absolute temperature, δ_1 and δ_2 are the solvent and polymer solubility parameter, respectively. Hansen used the following equation with $\alpha = 1$ for the calculation of Flory-Huggins intraction parameters,

$$\chi_{12} = \alpha \frac{Vs}{RT}[(\delta_{dS} - \delta_{dP})^2 + 0.25(\delta_{pS} - \delta_{pP})^2 + 0.25(\delta_{hS} - \delta_{hP})^2] \tag{10}$$

A low value of the Flory–Huggins interaction parameter ($\chi < 0.5$) indicates a high intensity of polymer-solvent interactions, and a good solubility of a polymer into a solvent. Given the Hansen solubility parameter, the cohesive energy can be divided into three parts derived from three types of interaction forces, including dispersive forces (E_d), polar forces (E_p), and hydrogen bonding forces (E_p), degining as follows [21],

$$E_{coh} = E_d + E_p + E_h \tag{11}$$

The coresponding equation for Hunsen solubility parameters can be calculated as follows,

$$\delta_t^2 = \delta_d^2 + \delta_p^2 + \delta_h^2 \tag{12}$$

Thus the distance between solubility parameter of PEBAX 3000 and dimethylacetamid can be calculated using the equation below [18],

$$\Delta\delta = [(\delta_{d,p} - \delta_{d,s})^2 + (\delta_{p,p} - \delta_{p,s})^2 + (\delta_{h,p} - \delta_{h,s})^2]^{1/2} \tag{13}$$

2.2.6. Gas Permeation Measurements

In general, gases can pass throught nonporous membrane by a solution-diffusion mechanism [22],

$$P = S \cdot D \tag{14}$$

Where P is permeability coefficent, S and D refer to solubility and diffusivity coefficents, respectively. The solubility is a thermodynamic parameter depending on some parameters, including size of a gas molecule, intermolecular intractions between penetrant and polymer, physical properties, and condensibility of sorbed penetrants. Conversely, the diffusivity is a kinetic parameter, and is a measure of how fast a penatrant diffuse through a nonporous membrane. This parameter depends on some parameters, including penetrant geometry, polymer-penetrant intraction, free volume of polymer matrix, and chain flexibilty of polymer. While the increment in penatrant size leads to the enhancement in solubility, it leads to the decrement in diffusivity. The ideal selectivity (α) for gas pairs of i and j can be determined using the following equation [16],

$$\alpha_{i/j}^* = \left(\frac{P_i}{P_j}\right) = \left(\frac{D_i}{D_j}\right) \times \left(\frac{S_i}{S_j}\right) \tag{15}$$

Where P_i and P_j are the permeability coefficients of pure gases i and j. Permeabilities of N_2, CO_2, and CH_4 were measured using a membrane gas separation unit which is exhibited in Figure **2**. The apparatus consists of a membrnae cell made form stainless steel with the permeation area of $16.3 cm^2$. In all experiments the feed pressure was set 6bar, and downstream pressure was remained at the atmospheric pressure. All permeation measurements were performed at 25 °C, and results of gas permeation experiments were recorded once a constant permeability was observed. It should be noted that just after permeation measurements, membranes were placed at vacuum oven. The following equation was used to determine the permeability,

$$P = \frac{Q \times l}{A \times (p_1 - p_2)} \tag{16}$$
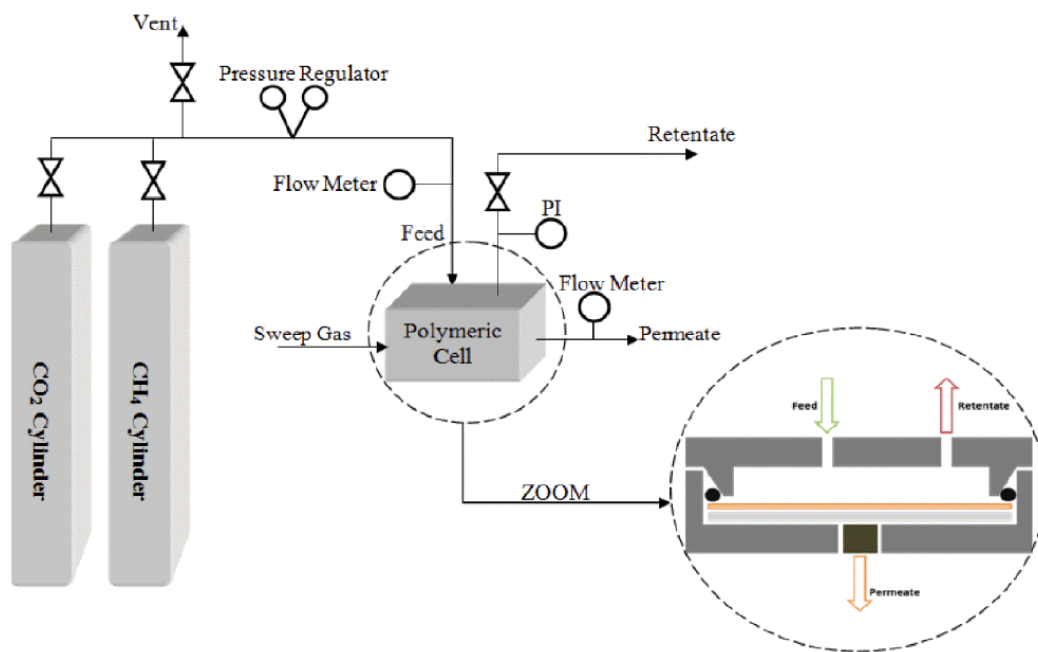
Figure 2: Schematic diagram of gas separation membrnae unit.

Where P is the permeability in barrer (1barrer $=10^{-10}$ cm^3 (STP) cm/cm^2.s. cmHg), Q is flow rate of the permeate gas (cm^3/s), I is the membrane thickness (cm), p_1 and p_2 stand for feed pressure (cmHg) and permeate pressure (cmHg), respectively, and A is the effective membrane area (cm^2).

3. RESULTS AND DISCUSSION

3.1. Density and Free Volume Determination

The additive model revealed that samples densities depend on the characteristics of polymer matrix. Densities of pristine PEBAX membranes and MMMs were determined using buoyancy method. Figure **3** compares experimental and theoretical densities of samples. As can be seen the rise in CSWCNTs content led to the increase in density of MMMs. The value of the experimental density for pristine PEBAX membrnae is 1.02g/cm^3. It is plainly visible that the values of the experimental densities for all the samples are marginally higher than those of theoretical densities. This is an indication that due to structural compleities all parameters cannot be considered in the theoretical calculations (e.g., inter/intramolecular forces and geometry of cavities) [17, 18].
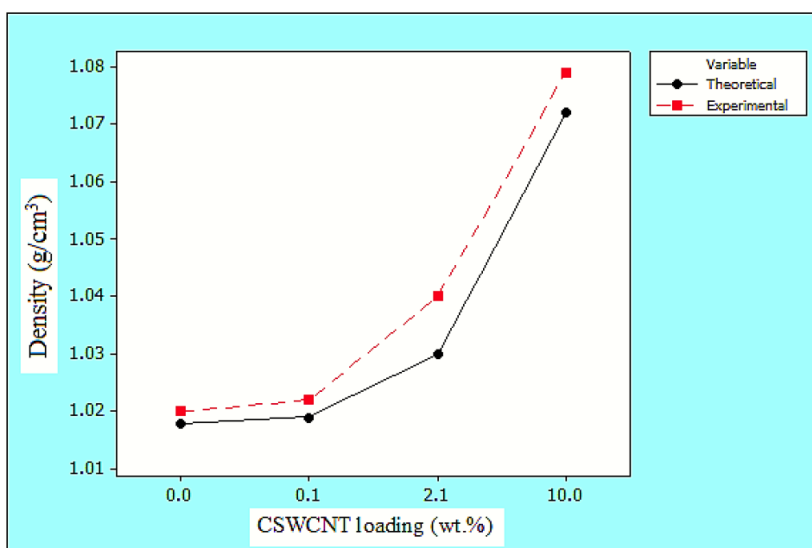
Figure 3: A comparison between theoretical and experimental densities as a function of CSWCNTs loading (wt%).
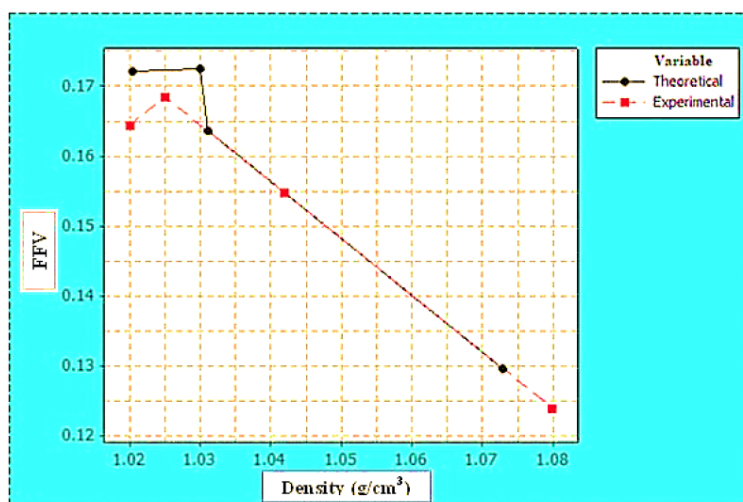
Figure 4: Fractional free volume as a function of theoretical and experimental densities.

Apart from a slight increase in both theoretical and experimental fractional free volume at the very low density values, the rise in densities of samples brought about the decline in both theoretical and experimental fractional free volume (Figure **4**).

The increment in figure of CSWCNTs nanofillers (0.1, 2.1, and 10 wt%) whitin MMMs can lead to the change in the cavities of PEBAX/CSWCNTs composite membranes. The obtained results can explain the appropriate intractions between the carboxylate groups of CSWCNTs with the functional groups available in PEBAX copolymer, resulting in penetration of the polymer chains inside cylinderical shaped CSWCNTs. The polymer chains can also embrace and surround CSWCNTs. These kinds of interactions can increase the packing density of the prepared membranes. The

results of the calculated parameters are presented in Table **2**.

3.2. Solubility Parameter Calculations

Table **3** represents the calculated parameters required for determination of solubility parameter of PEBAX/solvent and the value of Flory-Huggins interaction. The solubility parameter and Flory–Huggins interaction for PEBAX/NMP are observed to be smaller than those of PEBAX/DMAc. So it can be concluded that PEBAX/NMP gelation is rather faster than PEBAX/DMAc at room temperature. Given PEBAX/Ethanol system, due to the huge differnce between solubility parameters, and large value of Flory-Huggins interaction, this solvent seems to be inappropriate for membranes fabrication. PEBAX does

Table 2:   Fractional Free Volume Calculations

CSWCNTs loading (wt%)	CSWCNTs amount (gr)	ϕ_f	ρ additive (theoretical) (g. cm^{-1})	ρ experimental (g. cm^{-1})	FFV
0.1	0.0260	0.000485	1.0205	1.025	0.168
2.1	0.0557	0.010314	1.0311	1.0419	0.154
10	0.2800	0.049706	1.073	1.08	0.123

Table 3:   Physical Properties of PEBAX and Various Solvents

Type	δ_d (MJ/m^3)$^{1/2}$	δ_p (MJ/m^3)$^{1/2}$	δ_h (MJ/m^3)$^{1/2}$	δ_t (MJ/m^3)$^{1/2}$	$\Delta\delta$(MJ/m^3)$^{1/2}$	V_m (cm^3/mol)	χ_{12}
Pebax MV 3000	21.23	9.38	8.43	24.69			
NMP	18.0	12.3	7.2	22.95	4.52	96.5	0.32
DMAc	16.8	11.5	10.2	22.77	5.22	92.997	0.55
Ethanol	15.8	8.8	19.4	26.52	12.25	58.5	5.36

not dissolve in DMAc at room temperature, and prepared solution is stable only at elevated temperature. Hence the dissolution of PEBAX in DMAc was carried out at elevated temperature under reflux. The low value (0.55) of Flory-Huggins interaction confirms a suitable solubility of PEBAX and DMAc under reflux.

Intraction mechanism between polymer-solvent system can be categorized according to the orthogonal dipolar interactions among dipoles of amide C=O bond of carbonyl group (C=O·····C=O). Under reflux condition, DMAc (as solvent) can penetrate into the polymer chains, each of which has a helical-space conformation. Hydrogen bonding between polyamide and polyether chains breaks, dissolving of copolymer in the solvent [23]. In accordance with above explanation, DMAc was selected to prepare polymeric solution and other alternatives were eliminated.

3.3. Thermal Properties of Membranes

3.3.1. DSC Analysis

Table **4** represents data about the thermal properties of the samples measured using DSC thermograms. In Table **4**, pristine PEBAX membrane and composite membranes containing 0.1, 2.1, and 10wt% CSWCNTs are represented as PC_0, PC_1, PC_2, and PC_3, respectively. Except for membrane containing 10wt% CSWCNTs, the increment in amount of nanofillers in MMMs leads to the rise in melting temperature (T_m) of PE phase. What is more, the increase in T_m values of polyether phases of the membranes containing 0.1 and 2.1wt% nanofillers brings about the rise in rigidity and re-arrangement of the polyether phase of the polymer matrix. In the case of the membrane loaded by 10wt% CSWCNTs, T_m value declined, indicating high flexibility of polyether chains.

On the other hand, the increment in amount of nanofillers in MMMs caused the fall in T_m values of crystalline PA phases. The above results can refer to

the formation of the inter/intramolecular bonding between PA phase and CSWCNTs incorporated into the PEBAX matrix, resulting disordered arrangment in crystalline phase, which is responsible for the decline in T_m [24, 25].

Arrangment of the crystalline phase is, in part, distorted by the effect of CSWCNTs within the PA phase. Calculations confirmed that the degree of crystallinity of PE phase rose, when amount of CSWCNTs increased from 0.1 to 2.1wt% whereas crystallinity degree in the case of PEBAX/CSWCNTs 10wt% dropped to 3.02. The converse trend was observed in the case of PA phase, in other words, the rise in amount of nanofillers posed the decrease to the crystallinity degree of PA phase. It is due to the effect of highly loaded nanofillers whitin polymer matrix. Therefore, incorporation of 10wt% CSWCNTs can lead to higher flexibility of PA phase, and can result in creation of new defects in crystal lattice of PA phase. Thus, crystallinity degree of PA phase decreased from 21.22% to 12.60%. It is worth noting that incorporation of 10% of nanofillers has a positive effect on permselectivity of MMMs for CO_2/CH_4 separation. Figure **5** shows how introducing CSWCNTs to the PEBAX membranes can affect the crystallinity degrees of PE and PA phases [25, 26].

3.3.2. TGA Analysis

Thermal resistance of pristin membrnaes and MMMs were investigated using thermogravimetric analysis (Figure **6**). Degradation temperatures of pristine PEBAX and composite membranes are just before 400°C. There are no significant weight losses at temperatures below about 400°C. Both pristine PEBAX and composite membranes have weight losses <10% at temperatures below 400°C. The main reason for this observation can be referred to the early decomposition of impurities, such as water and low molecular weight polymers within the samples [1,8,22]. The main weight loss for all of the samples occurs at the temperatures between 400 °C and 500 °C. To put it another way, the increment in temperature provides the necessary

Table 4:   Thermal Properties and Crystallinity of PEBAX Membranes with Different CSWCNTs Content

Sample	CSWCNTs (wt%)	T_m (PE) (°C)	T_m (PA) (°C)	ΔH_f (PE) (Jg^{-1})	ΔH_f (PA) (Jg^{-1})	X_c (%) (PE)	X_c (%) (PA)
PC_0	0	68.416	161.333	2.365	20.798	2.00	21.22
PC_1	0.1	72.670	157.337	2.873	19.397	2.43	19.70
PC_2	2.1	80.337	157.004	3.875	15.550	3.28	15.79
PC_3	10	74.933	153.600	3.572	12.412	3.02	12.60
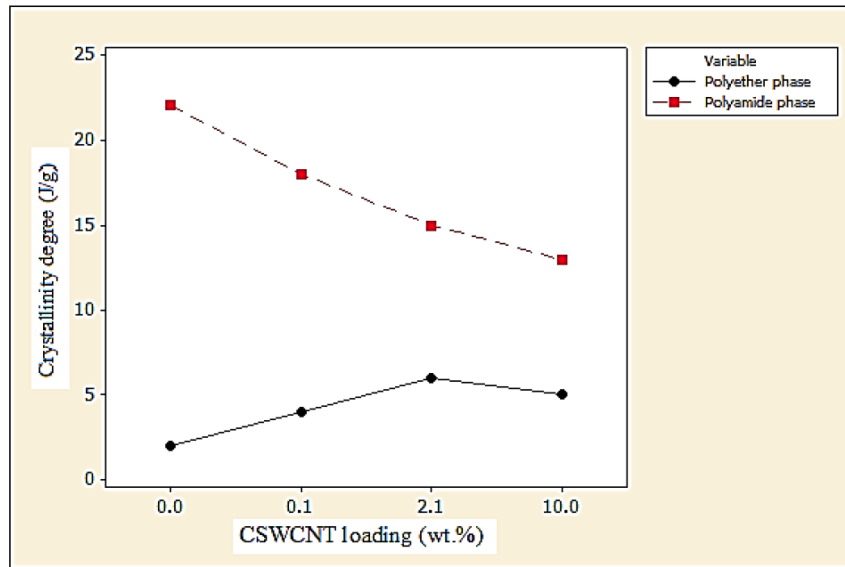
**Figure 5:** Effect of nanofillers content on crystallinity degree of PE and PA phases.

energy for molecular dissociation of polymer chains. According to the results, approximately similar thermal stabilities of PEBAX membranes are observed.

Regarding Figure **6**, it is plainly visible that the rise in figure of nanofillers led to the less weight losses in the last part of thermal degradation curves beginning at 500 °C. It can be attributed to the higher carbon contents in MMMs compairing that of pristine membrane.

3.4. Contact Angle Measurements

The changes in contact angle of the pristine PEBAX membrane and MMMs (containing 10% CSWCNTs) as

a function of time are shown in Figure **7**. As can be seen, the increment in experiment time, led to the decrease in contact angle of both pristine PEBAX membrane and MMMs, leading to the increase in the relative cohesiveness and intraction of the solid sample with water molecules. The expected increase in the critical surface tension is accompanied with stronger adsorptive behavior [27]. The surface hydrophilicity of MMMs (containing 10wt% CSWCNTs) is far more that that of pristine PEBAX membrnae. The enhanced surface wettability of the these samples can be attributed to the effect of CSWCNTs loading on the surface polarity of the membranes, and suitable relative cohesiveness of the solid sample with water molecules.
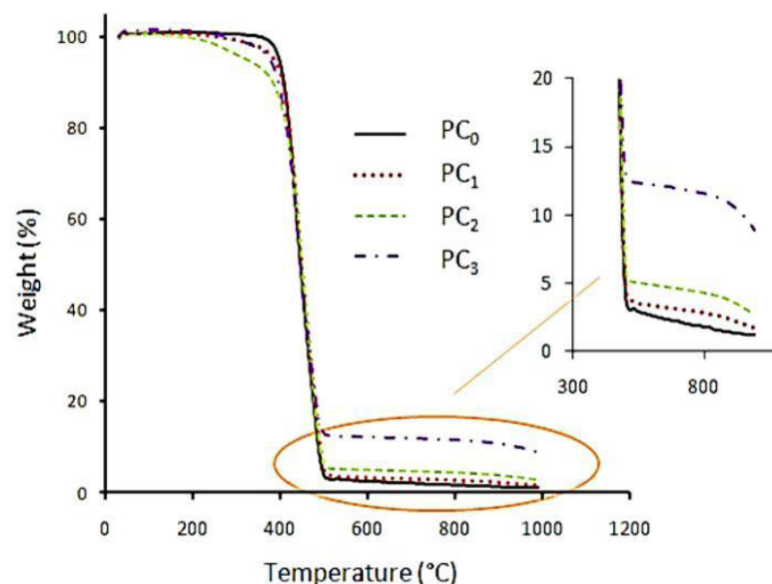
Figure 6: Thermal degradation curves of PEBAX membranes and MMMs.
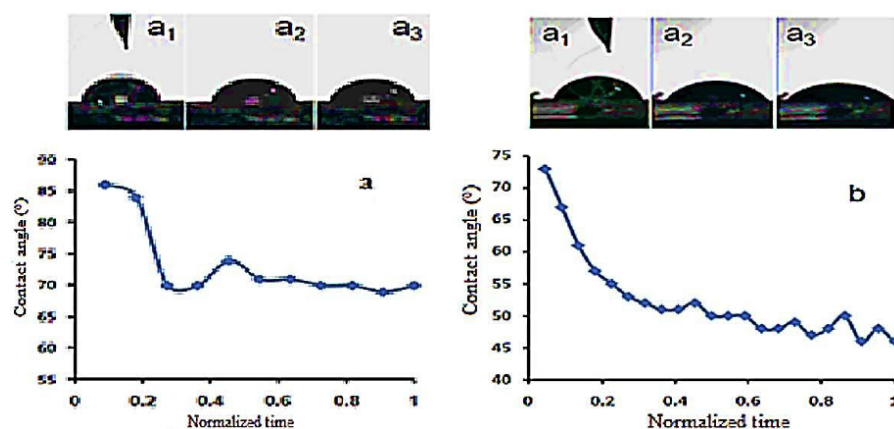
Figure 7: surface contact angle of **a**) pristine PEBAX membrane and **b**) MMMs (containing 10wt% CSWCNTs).

3.5. FTIR Analysis

Functional groups and inter/intramolecular interactions were investigeted using FTIR spectroscopy. Figure **8** represents the FTIR spectra of the pristine PEBAX membrane and MMMs (containing 10wt% CSWCNTs) membranes. In the case of pristine PEBAX membrane, the band at 1110cm^{-1} stands for the stretching vibrations of ether groups (C-O-C), and the band appeared at 1564cm^{-1} is responsible for the bending vibration of N-H group. The band which is responsible for the stretching vibration of carbonyl groups in an amide group (H-N-C=O) appeared at 1641cm^{-1} while the stretching vibration of carbonyl group in the state of carbonyl associated with ether oxygen (O-C=O) appeared at 1737cm^{-1}. The absorption frequency of O-C=O group compared to that of H-N-C=O group is higher, it can be attributed to the higher electron-withdrawing effect (inductive effect) of O-C=O than that of H-N-C=O. In fact, the higher electron-withdrawing property of oxygen atoms in comparison with that of nitrogen atoms led to the stronger bonds and higher force constant (K) of the carbonyl groups in O-C=O groups compared to those of H-N-C=O groups [26].

Two bands located at 2852cm^{-1} and 2921cm^{-1} stand for presence of the aliphatic C-H connected to the amide group (H-C-CONH), and also the band at 3094cm^{-1} is related to the presence of the aliphatic C-H connected to the ether group (C-O-C-C-H). The absorption band at 3296cm^{-1} corresponds to the N-H group. Loading of 10wt% nanofillers within polymer matrix caused a decrease in force constent (K). Consequently absorbance bands of C-O-C, N-H, and H-N-C=O functional groups shifted to the lower frequencies. These changes can be attributed to the intermolecular hydrogen-bondings between the carboxylic group of SWCNT nanofillers and N-H group of polyamide segments. In fact the crystallinity of hard segments of polyamide was reduced.
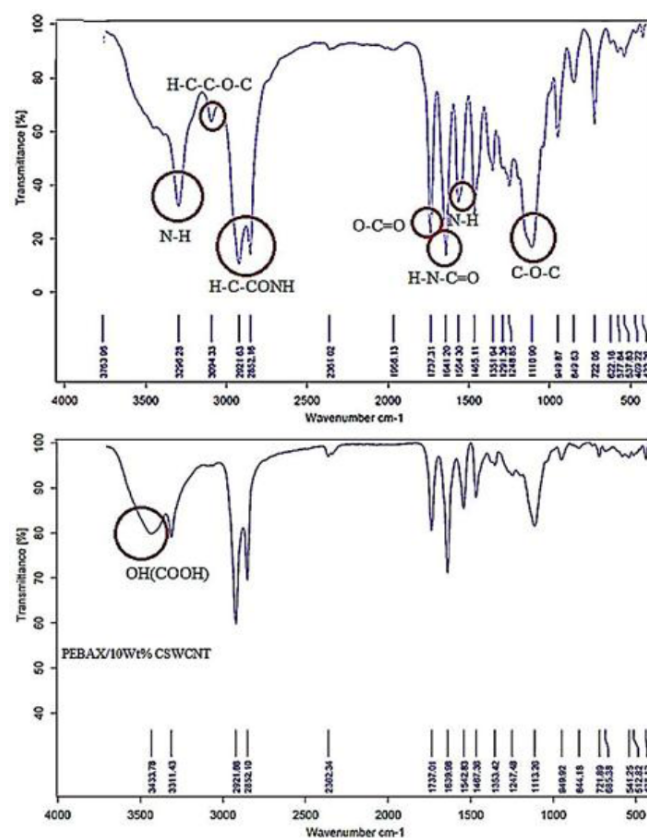
Figure 8: FTIR spectra of pristine PEBAX membrane (upper spectrum), and MMMs containing 10wt% CSWCNTs (lower spectrum).

Two vibration bands at 3397cm^{-1} and 3433cm^{-1} stand for the hydrogen-bondings of OH groups in CSWCNTs nanofillers [28]. Figure **9** demonstrates schematic representation of intermolecular hydrogen bonding between amine group in a PEBAX copolymer and carboxylic group a CSWCNT.
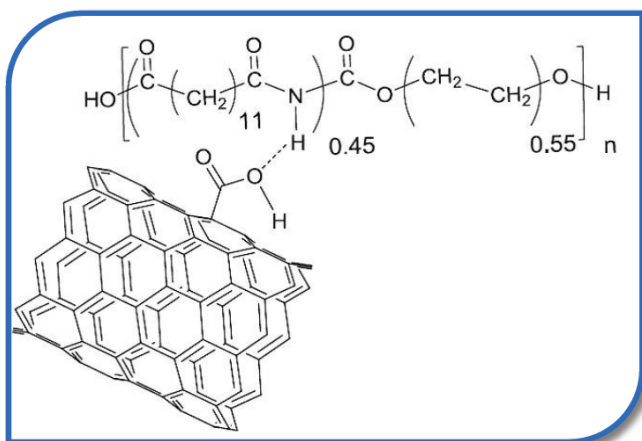
Figure 9: Schematic representation of intermolecular hydrogen bonding between amine group in a PEBAX copolymer and carboxylic group in a CSWCNTs.

3.6. Morphology Studies of PEBAX Membranes

Figure **10** depicts pristine PEBAX membranes and two types of MMMs.
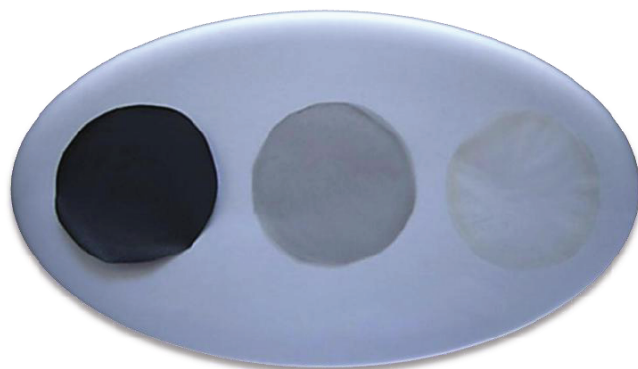
Figure 10: Pristine PEBAX membrane (right), MMMs containing 0.1wt% CSWCNTs (middle), and MMMs containing 10wt% CSWCNTs (left).

3.6.1. AFM Characterization

AFM images provide useful information about surface topography, and segments orientation of both polyether and polyamide phases (Figure **11**). Regarding Figure **11a**, the brighter areas correspons to the PA phase (crystalline regions of PEBAX). The PA phases are surrounded by PE phases (darker areas) [17]. Figure **11b** represents the effect of nanofillers on the surface morphology of the MMMs (containing 10wt% CSWCNTs). In fact, nanofillers incorporation into polymer matrix led to the formation of closer-packed polymer matrices compared those of pristine PEBAX membranes. The periodic lattices with irregular organization and dark border, which is due to good compatibilty of CSWCNTs with polymer chains, can be observed in Figure **11b** [29,30].

3.6.2. SEM-EDX Characterization

The cross-section SEM images of MMMs (containig 10wt% CSWCNTs) are depicted in Figure **12**. These images symbolize a suitable combination and adhesion between PEBAX and CSWCNTs particles. The incorporation of nanofillers into PEBAX matrix results in the formation of microvoids at the polymer-sieves interfaces. Table **5** shows the quantitative microanalysis of the pristine PEBAX membranes and MMMs (containing 10wt% CSWCNTs). The quantitative microanalysis of oxygen and nitrogen atoms clearly indicate the diffusion of CSWCNTs nanofillers within elemental components of the polymer matrix [31].

According to the results indicated in Table **5**, while apparent concentration of carbon atoms in pristine PEBAX membranes is 140.21, it is 118.90 in MMMs (containing 10wt% CSWCNTs). To put it another way, incorporation of nanofillers into polymer matrix led to the considerable decrease in apparent concentration of carbon atoms in MMMs. However, the opposite holds true nitrogen and oxygen atoms. When it comes to the intensity ratio of atoms, it is plainly visible that incorporation of CSWCNTs into polymer matrix resulted in the fall in intensity ratio of carbon, whereas intensity ratio of both nitrogen and oxygen atoms increased. When nanofillers were introduced to the pritine PEBAX membranes, weight percent of oxygen atom grew from 13.37% to 20.27%. Furthermore, the value of atomic percent increased to 16.67% for the case of oxygen atoms, whereas this value for both carbon and nitrogen atoms decreased.

The microanalysis spectra of both pristine PEBAX membranes and MMMs (containing 10wt% CSWCNTs) are exhibited in Figure **13**. The EDX mapping images of the surface morphology of pristine PEBAX membranes and PEBAX/CSWCNTs (10 wt%) membranes are represented in Figures **14** and **15**, respectively.

As can be clearly observed in Figure **15**, nanofillers are distributed finely and randomly throughout the membrane matrix. Given Figures **14d** and **15d**, the brighter and the darker areas indicate the microphase separation occurred within the polymer matrix, which is a common characteristic of PEBAX copolymer. Whereas the brighter areas corrospond to the PE phase, the darker regions, which are randomly distributed in polymer matrix, stand for the crystalline PA phase [31].
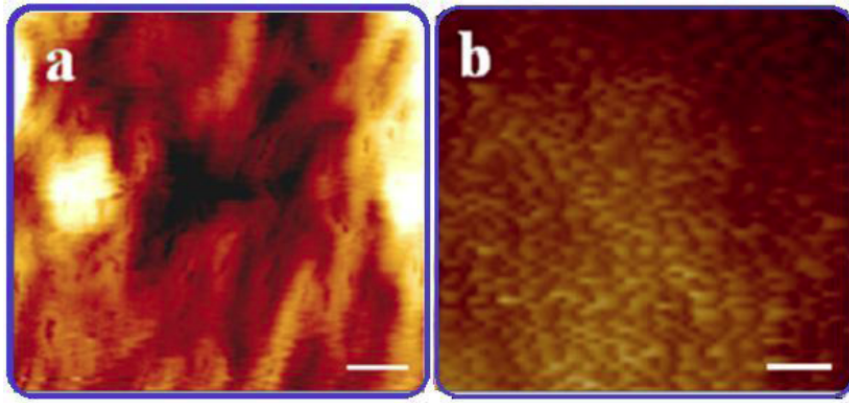
Figure 11: AFM images from surface of membranes **a**) pristine PEBAX membrane, and **b**) MMMs containing 10wt% CSWCNTs (All scale bars represent 10nm).
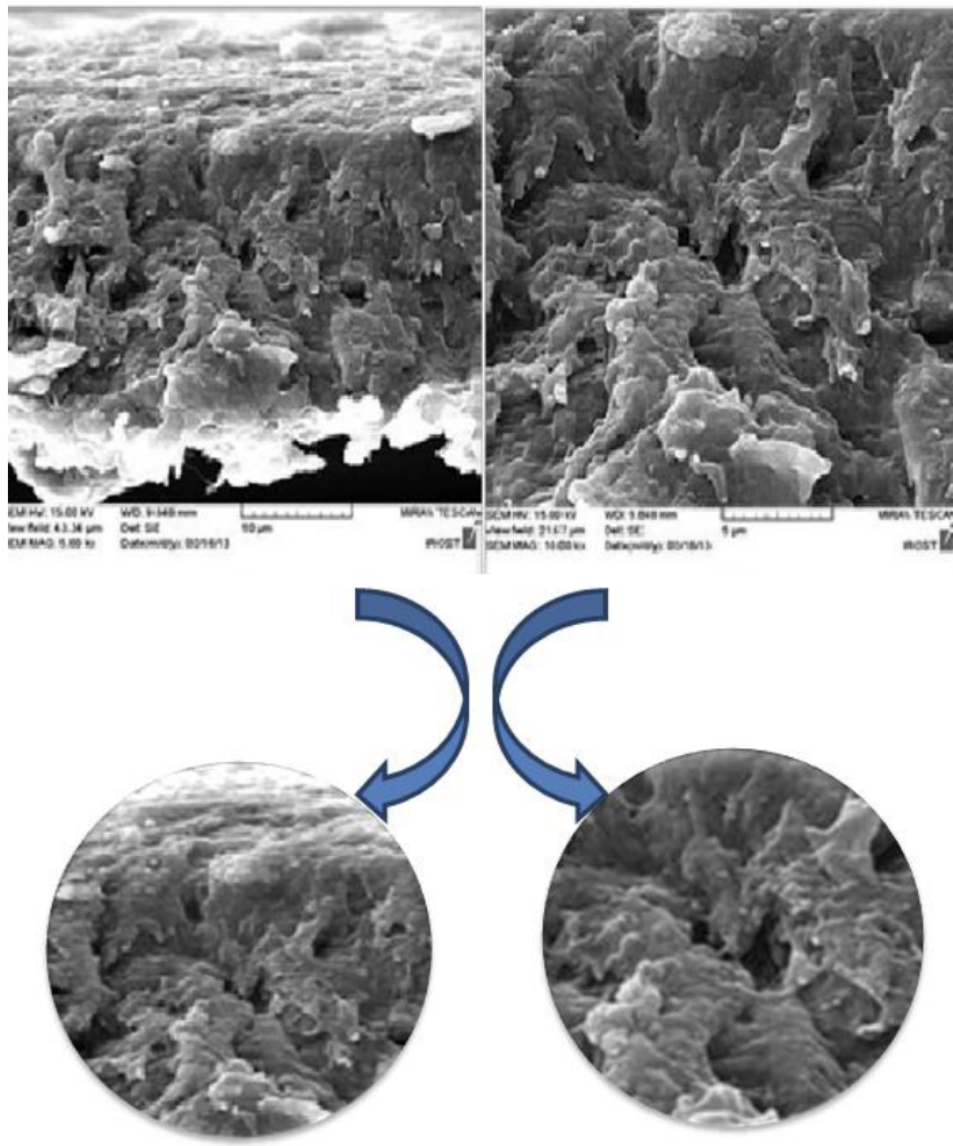

Figure 12: Cross-section SEM images of MMMs (containing 10wt% CSWCNTs).

Table 5:   Quantitative Elemental Analysis of Upper Surface of Pristine PEBAX Membrane and MMMs (Containing 10wt% CSWCNTs)

Type	Element	App Conc.	Intensity Corrn.	Weight%	Weight% Sigma	Atomic%
Pristine PEBAX membrnaes	C Kα	140.21	1.6116	59.62	3.47	64.23
	N Kα	3.66	0.0928	27.02	4.17	24.96
	O Kα	5.86	0.3002	13.37	1.23	10.81
	Total			100.00	100.00	
MMMs (containing 10wt% CSWCNTs)	C Kα	118.90	1.5047	53.87	2.21	59.03
	N Kα	3.93	0.1036	25.86	2.97	24.30
	O Kα	9.79	0.3292	20.27	1.04	16.67
	Total			100.00	100.00	
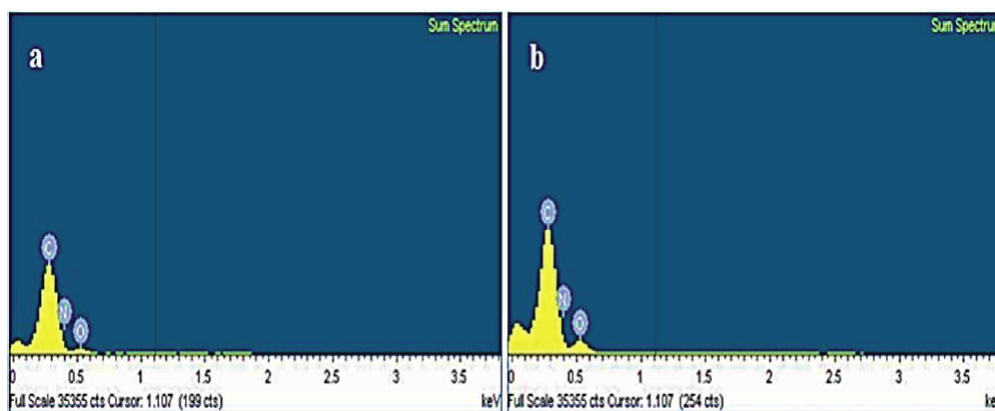
Figure 13: Histogram of intensity versus voltage, **a**) pristine PEBAX membranes, **b**) MMMs (containing 10wt% CSWCNTs).
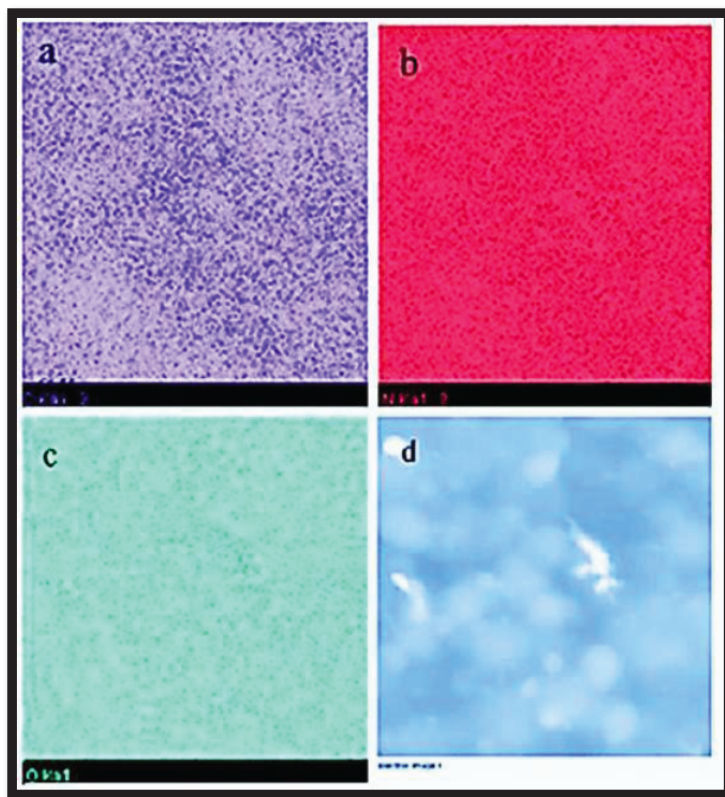
Figure 14: EDX-SEM mapping images of pristine PEBAX membranes. **a**, **b**, and **c**) representative of carbon Kα1, nitrogen Kα1, and oxygen Kα1, respectively, and **d**) electron image.
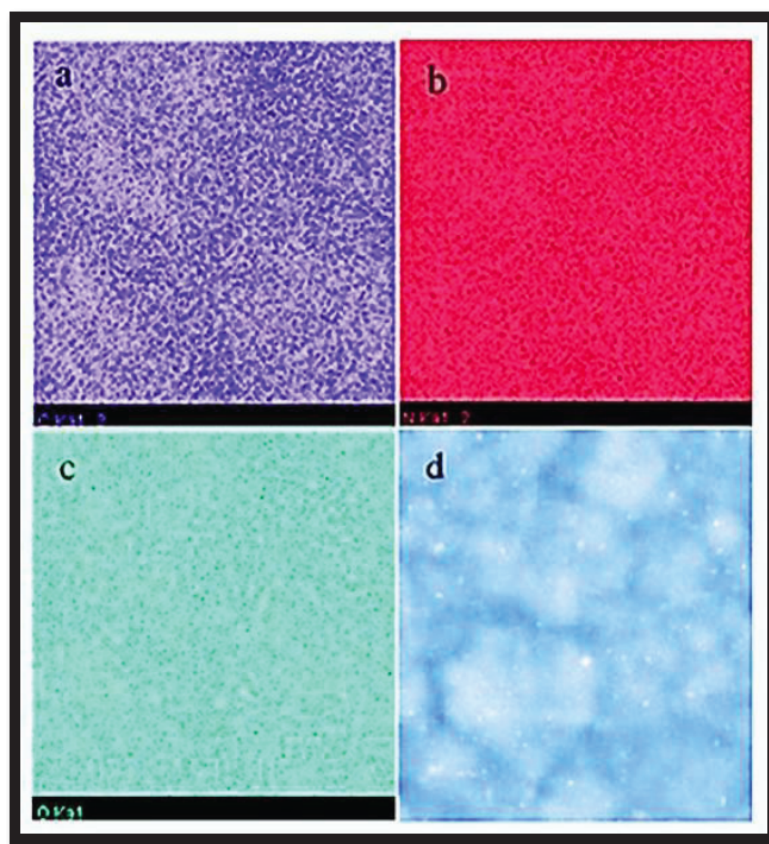
Figure 15: EDX- SEM mapping images of MMMs (containing 10wt% CSWCNTs). **a**, **b**, and **c**) representative of carbon Kα1, nitrogen Kα1, and oxygen Kα1, respectively, and **d**) electron image.
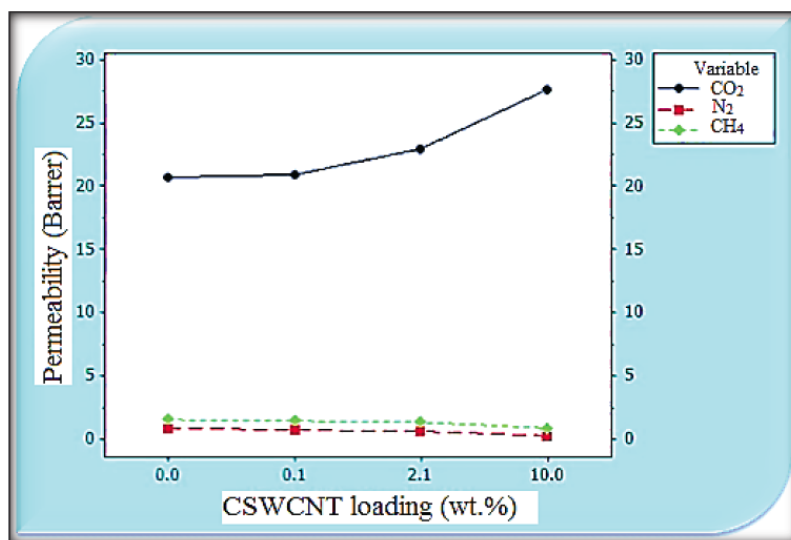
3.7. Effect of CSWCNTs Loading on Permselectivity of PEBAX Membranes

PEBAX membranes filled with CSWCNTs show an improved selectivity of both CO_2/N_2 and CO_2/CH_4. Since PEBAX copolymer is consist of immiscible parts, this block copolymer is known for indication of microphase-separated structures [13]. The PA segment provides a mechanical stability for the film whereas the PE segment due to the its mobility, provides sites for the film through which gases can permeate [14]. PEBAX membranes have particularly a high gas separation capability, an illustration for that is separation of CO_2 from N_2 or CH_4. It has been reported that the high CO_2/N_2 selectivity can be referred to the high solubility of CO_2, which is a highly polarizable gas [32].

PEBAX membranes indicate a nonpolar/polarizable-based gas separation property, making these class of membranes applicable for separation of polarizable gases, such as CO_2 and H_2S from nonpolar gases (N_2 and CH_4). As shown in Figure **16**, the increment in polar carboxyl functionalities within PEBAX matrix by adding CSWCNTs to polymer matrix, can give the interactions between PE blocks of the polymer nanocomposite and CO_2 gas a boost [15,16]. Hence, introducing CSWCNTs to pristine PEBAX membranes let to the growth in CO_2 permeability. Nonpolar gases (N_2 or CH_4), on the other hand, could not interact with polarized site of MMMs, that is all the more reason why the permeability of nonpolar gases through MMMs undergone a decrement. The steric correlations between carboxyl groups of nanofillers and -C=O, -N-H, and -O-C-C-O- groups in PEBAX chains can also make an improvement in permeability of CO_2.

Higher CO_2/N_2 and CO_2/CH_4 selectivity values can be obtained by increasing the CSWCNTs content (see Figure **17**). Nanofillers possessing polar groups can affect the solubility selectivity of polar gases. As a matter of fact, incorporation of CSWCNTs into the polymer matrix led to the increase in permeability of CO_2, due to the polar nature of CSWCNTs. The increase in ideal selectivity can be explained by the effect of nanofillers on the solubility and diffusivity coefficients. In the case of diffusivity coefficient, the increase in the proportion of nanofillers within polymer matrix posed the decline in FFV of MMMs, causing the drop in diffusivity coefficient for CO_2, N_2, CH_4 [33].

Figure 16: The effect of CSWCNTs loading on permeability properties of CO_2, CH_4, and N_2 gases (feed pressure of 6 bar).
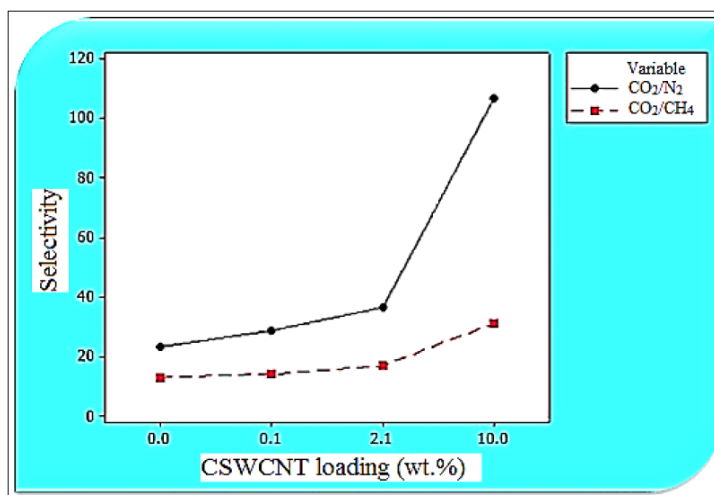
Figure 17: Ideal selectivity of MMMs as a function of nanofillers loading.

MMMs with higher proportion of polar groups exhibited an increase in CO_2 solubility coefficient whereas this parameter for N_2 and CH_4 gases decreased compared to that of pristine PEBAX membranes. The higher value of CO_2 solubility coefficient can be attributed to the quadrupole moment of CO_2, which is way higher than those of CH_4 and N_2 as non-polar gases [17, 18, 34].

Table **6** represents the permeability results of pristine PEBAX membrane and MMMs (containing 0.1, 2.1, and 10wt% CSWCNTs, represented as PC_0, PC_1, PC_2, and PC_3, respectively). Despite the higher value of quadrupole moment of N_2 compared to that of non-palar CH_4 gas, the higher permeability of CH_4 can be attributed to its large potential parameter (e/k_B= 158.5 K) [34, 35]. The selectivity results of CO_2/N_2 and CO_2/CH_4 are also prepsented in Table **6**. No

remarkable transformations in selectivity were observed, irrespective of MMMs containing 10wt% CSWCNTs. However, a considerable improvement in selectivity can be distinguished in the case of MMMs containing 10wt% CSWCNTs. The ideal selectivity rose from 23.3 to 106.4 for CO_2/N_2, and for CO_2/CH_4 this factor increased from 13.2 to 31.3.

4. CONCLUSION

In the present study, the effect of CSWCNTs on the CO_2/N_2 and CO_2/CH_4 selectivities were investigated. PEBAX matrix was modified by incorporating nanofillers into polymer matrix. Nanofillers with polar properties were applied in order to enhance the permeation of CO_2 (as a polar gas) versus CH_4 and N_2 (as non-polar gases). Incorporation of CSWCNTs nanofillers into polymer matrix not only can increase

Table 6:   Gas Permselectivity Datas for PEBAX Membranes Filled with Different CSWCNTs Content

Sample	P (CO_2) (Barrer)	P (N_2) (Barrer)	P(CH_4) (Barrer)	α (CO_2/N_2)	α (CO_2/CH_4)
PC_0	39.7	1.7	3.0	23.3	13.2
PC_1	40.1	1.4	2.8	28.6	14.3
PC_2	44.1	1.2	2.6	36.7	17.0
PC_3	53.2	0.5	1.7	106.4	31.3

the polarizability, but also can rise the solubility capacity, which is a great approach to attain highly selective membranes for polar/nonpolar gas separation. In other words, Incorporation of polar inorganic nanofillers into the polymer matrix resulted in more solubility of CO_2 (as a polar gas), and less solubility of N_2 or CH_4 (as non-polar gases) in the MMMs.

Nevertheless, introducing nanofillers to the polymer matrix declined FFV values, and gas diffusivity through MMMs dropped accordingly. While permeation of N_2 and CH_4 dropped by increasing CSWCNTs content in MMMs, CO_2 permeation constantly increased, leading to the rise in CO_2/CH_4 and CO_2/N_2 selectivities. The approach described in this work is an effective method for polar and nonpolar gases separation.

ACKNOWLEDGEMENT

REFERENCES

[1]   Rahmani M, Kazemi A, Talebnia F. Matrimid mixed matrix membranes for enhanced CO2/CH4 separation. J Polym Eng 2016; 36: 499-511.
https://doi.org/10.1515/polyeng-2015-0176

[2]   Azizi N, Mohammadi T, Behbahani RM. Comparison of permeability performance of PEBAX-1074/TiO2, PEBAX-1074/SiO2 and PEBAX-1074/Al2O3 nanocomposite membranes for CO2/CH4 Separation. Chem Eng Res Des 2017; 117: 177-189.
https://doi.org/10.1016/j.cherd.2016.10.018

[3]   Jusoh N, Yeong YF, Lau KK, Shariff AM. Enhanced gas separation performance using mixed matrix membranes containing zeolite T and 6FDA-durene polyimide. J Membr Sci 2017; 525: 175-186.
https://doi.org/10.1016/j.memsci.2016.10.044

[4]   Martin-Gil V, López A, Hrabanek P, Mallada R, Vankelecom IFJ, Fila V. Study of different titanosilicate (TS-1 and ETS-10) as fillers for Mixed Matrix Membranes for CO2/CH4 gas separation applications. J Membr Sci 2017; 523: 24-35.
https://doi.org/10.1016/j.memsci.2016.09.041

[5]   Peng D, Wang S, Tian Z, Wu X, Wu Y, Wu H, Xin Q, Chen J, Cao X, Jiang Z. Facilitated transport membranes by incorporating graphene nanosheets with high zinc ion loading for enhanced CO2 separation. J Membr Sci 2017; 522: 351-362.
https://doi.org/10.1016/j.memsci.2016.09.040

[6]   Boroglu MS, Yumru AB. Gas separation performance of 6FDA-DAM-ZIF-11 mixed-matrix membranes for H2/CH4 and CO2/CH4 separation. Sep Purif Technol 2017; 173: 269-279.
https://doi.org/10.1016/j.seppur.2016.09.037

[7]   Sun H, Wang T, Xu Y, Gao W, Li P, Niu QJ. Fabrication of polyimide and functionalized multi-walled carbon nanotubes mixed matrix membranes by in-situ polymerization for CO2 separation. Sep Purif Technol 2017; 177: 327-336.
https://doi.org/10.1016/j.seppur.2017.01.015

[8]   Rahmani M, Kazemi A, Talebnia F, Gamali PA. Fabrication and characterization of brominated matrimid® 5218 membranes for CO2/CH4 separation: application of response surface methodology (RSM). e-polymers 2016; 6: 481-492.
https://doi.org/10.1515/epoly-2016-0140

[9]   Hibshman C, Cornelius CJ, Marand E. The gas separation effects of annealing polyimide-organosilicate hybrid membranes. J Membr Sci 2003; 211: 25-40.
https://doi.org/10.1016/S0376-7388(02)00306-X

[10]   Suzuki T, Yamada Y. Physical and gas transport properties of novel hyperbranched polyimide-silica hybrid membranes. Polym Bull 2005; 53: 139-146.
https://doi.org/10.1007/s00289-004-0322-9

[11]   Abbasszadeh Gamali P, Kazemi A, Zadmard R, Jalali Anjareghi M, Rezakhani A, Rahighi R, Madani M. Distinguished discriminatory separation of CO2 from its methane-containing gas mixture *via* PEBAX mixed matrix membrane, Chinese Journal of Chemical Engineering, in press.
https://doi.org/10.1016/j.cjche.2017.04.002

[12]   Patel NP, Zielinski JM, Samseth J, Spontak RJ. Effects of pressure and nanoparticle functionality on CO2-selective nanocomposites derived from crosslinked poly(ethylene glycol). Macromol Chem Phys 2004; 205: 2409-2419.
https://doi.org/10.1002/macp.200400356

[13]   Liu L, Chakma A, Feng X. A novel method of preparing ultratin poly(ether block amide) membranes. J Membr Sci 2004; 235: 43-52.
https://doi.org/10.1016/j.memsci.2003.12.025

[14]   Barbi V, Funari SS, Gehrke R, Scharnagl N, Stribeck N. SAXS and gas transport in poly(ether-block-polyamide) copolymer membranes. Macromolecules 2003; 36: 749-758.
https://doi.org/10.1021/ma0213403

[15]   Kim JH, Ha SY, Lee YM. Gas permeation of poly(amide-6-*b*ethylene oxide) copolymer. J Membr Sci 2001; 190: 179-193.
https://doi.org/10.1016/S0376-7388(01)00444-6

[16]   Lin H, Freeman BD. Materials selection guidelines for membranes that remove CO2 from gas mixtures. J Mol Struct 2005; 739: 57-74.
https://doi.org/10.1016/j.molstruc.2004.07.045

[17]   Yumpolskii Y, Freeman BD. Membrane gas separation. John Wiley & Sons 2010.

[18]   Car A, Stropnik C, Yave W, Peinemann K. PEG modified poly(amide-*b*-ethylene oxide) membranes for CO2 separation. J Mem Sci 2008; 307: 88-95.
https://doi.org/10.1016/j.memsci.2007.09.023

[19]   Van Krevelen DW. Properties of polymers: their correlation with chemical structure, their numerical estimation and prediction from additive group contributions. 3rd ed. Elsevier: New York, 1990; p. 875.

[20]   Hildebrand J, Scott RL. The Solubility of Nonelectrolytes, 3rd ed., Reinhold, New York 1950.

[21]   Hansen CM. Hansen solubility parameter, Handbook, second edition, CRC 2007.

[22]   Rahmani M, Kazemi A, Talebnia F, Khanbabaei G. Preparation and characterization of cross-likned matrimid membaranes for CO2/CH4 separation. Polym Sci Ser B 2014; 56: 650-656.
https://doi.org/10.1134/S1560090414050108

[23]   Dasgupta S, Hammond WB, Goddard WA. Crystal Structures and Properties of Nylon Polymers from Theory. J Am Chem Soc 1996; 118: 12291-12301.
https://doi.org/10.1021/ja944125d

[24]   Archondouli PS, Kalfoglou NK. Compatibilization and properties of PBT/PU polymeric alloys. Polymer 2001; 42: 3489-3502.
https://doi.org/10.1016/S0032-3861(00)00758-8

[25]   Hu CB, Ward RS, Schneider NS. A new criterion of phase separation: the effect of diamine chain extenders on the properties of polyurethane ureas. J Appl Polym Sci 1982; 27: 2167-2177.
https://doi.org/10.1002/app.1982.070270627

[26]   Mayo SL, Olafson BD, Goddard WA. A Generic Force Field for Molecular Simulations. J Phys Chem 1990; 94: 8897-8909.
https://doi.org/10.1021/j100389a010

[27]   Tutak W, Chhowalla M, Sesti F. The chemical and physical characteristics of single-walled carbon nanotube film impact on osteoblastic cell response. Nano Tech 2010; 21: 315102.
https://doi.org/10.1088/0957-4484/21/31/315102

[28]   Pavia DL, Lampman GM, Kriz GS. Introduction to spectroscopy, Thomson learning 2001.

[29]   Magonov SN, Reneker DH. Characterization of polymer surfaces with atomic force microscopy. Annu Rev Mater Sci 1997; 27: 175-222.
https://doi.org/10.1146/annurev.matsci.27.1.175

[30]   Dasgupta S, Hammond WB, Goddard WA. Crystal Structures and Properties of Nylon Polymers from Theory. J Am Chem Soc 1996; 118: 12291-12301.
https://doi.org/10.1021/ja944125d

[31]   Corneala LM, Mastenb SJ, Daviesb SHR, Tarabarab VV, Byunb S, Baumann MJ. AFM, SEM and EDS characterization of manganese oxide coated ceramic water filtration membranes. J Membr Sci 2010; 360: 292-302.
https://doi.org/10.1016/j.memsci.2010.05.026

[32]   Bondar VI, Freeman BD, Pinnau I. Gas transport properties of poly(ether-*b*-amide; segmented block copolymers. J Polym Sci Part B Polym Phys 2000; 38: 2051-2062.
https://doi.org/10.1002/1099-0488(20000801)38:15<2051::AID-POLB100>3.0.CO;2-D

[33]   Gomes D, Nunes SP, Peinemann KV. Membranes for gas separation based on poly(1-trimethylsilyl-1-propyne)-silica nanocomposites. J Membr Sci 2005; 246: 13-25.
https://doi.org/10.1016/j.memsci.2004.05.015

[34]   Li Y, Chung TS. Highly selective sulfonated polyethersulfone (SPES)-basedmembranes with transition metal counterions for hydrogen recovery and nat-ural gas separation. J Membr Sci 2008; 308: 128-135.
https://doi.org/10.1016/j.memsci.2007.09.053

[35]   Buckingham AD, Disch RL, Dunmur DA. Quadrupole moments of some simple molecules. J Am Chem Soc 1968; 90: 3104-3107.
https://doi.org/10.1021/ja01014a023